

# Fracture Behavior and Morphology of Spun Collagen Fibers

KAZUHIKO TAKAKU, TAKEMITSU OGAWA, TAKASHI KURIYAMA, and IKUO NARISAWA\*

Department of Materials Engineering and Science, Yamagata University, College of Engineering,  
4-3-16 Jonan, Yonezawa-city, 992, Japan

## SYNOPSIS

The influence of glutaraldehyde (GA) crosslinking, basic chromium sulfate (Cr) tanning, and thermal treatments on the fracture behavior and morphology of spun collagen fibers has been studied. The fracture morphology of the fibers is characterized by longitudinal splitting along the fiber axis. Although the essential fracture morphology was not influenced by GA crosslinking, Cr tanning, and thermal treatments, the process of splitting depended on the kind of crosslink. Noncrosslinked and Cr-tanned fibers were split into fibrils, but GA-crosslinked fiber was split without fibrillation. The thermal treatments have two effects: One is decrease in number of defects and/or flaws; the other is gelatinization. In the thermal treatment above 140°C, the gelatinization plays a more important role for the tensile properties than does the effect of a decrease of a defect. Gelatinization results in the enhancements of slippage and separation of macrofibrils and/or fibrils after the yield point. © 1996 John Wiley & Sons, Inc.

## INTRODUCTION

The spun collagen fiber, which is the strongest among protein fibers,<sup>1</sup> is a kind of man-made protein fiber. There have been many studies in the 1930s on the protein fibers to make silk from natural proteins such as casein, soybean, corn, and peanut.<sup>2</sup> Besides, the spun collagen fibers were studied to apply to a surgical suture to utilize the byproducts in the leather industry.<sup>3-6</sup> Nevertheless, at the present time, the industrialization of protein fibers made from natural proteins is still not successful because of the insufficient mechanical properties for a practical use.

The structure, properties, and fracture morphology of natural collagen fibers such as rat tail tendon (RTT) were discussed in some reviews<sup>8,9</sup> and many reports.<sup>7-15</sup> There have been some articles discussing the influence of extraction rate, time of coagulation, coagulation agents, and glutaraldehyde (GA) crosslink on the tensile strength of spun collagen fiber.<sup>5,6</sup> For example, Harmed and Rodriguez reported that both crosslinking and scission reactions compete

with each other during irradiation.<sup>16</sup> Schimpf and Rodriguez described that tensile strength shows the maximum value when the fibers are treated at 0.2% GA concentration and then decreases due to the competing crosslink and chain scission mechanisms.<sup>5</sup> The structure and mechanical properties of the collagen fiber from pepsin-soluble collagen were also reported by Utsuo and Taniguchi.<sup>3,4,17</sup>

However, there has been no detailed studies on the fracture mechanism of the spun collagen fibers from a viewpoint of fracture morphology comparing GA-crosslinked fibers with basic chromium sulfate (Cr) tanning fibers. The purpose of this article was to investigate the influence of GA crosslinking, Cr tanning, and thermal treatments on the fracture behavior and morphology of the collagen fibers spun from alkaline-soluble collagen.

## EXPERIMENTAL

### Preparation of Collagen Solution

As the method of preparing collagen solution was described in detail elsewhere,<sup>18</sup> this will be only briefly described here. The hide was soaked, limed, and unharied. The limed hide was fleshed and split and then delimed and cut. An alkaline treatment

\* To whom correspondence should be addressed.

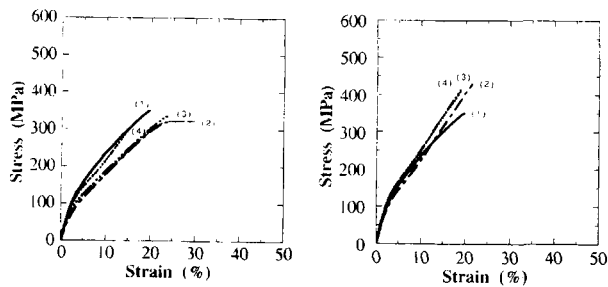


**Figure 1** The stress-strain curves of GA-crosslinked and Cr-tanned fibers. (a) GA-crosslinked fibers: (1) non-crosslinked (before GA-crosslinking treatment); (2) 0.1 wt % GA-crosslinked; (3) 1 wt % GA-crosslinked; (4) 3 wt % GA-crosslinked. (b) Cr-tanned fibers: (1) noncross-linked (before Cr-tanning treatment); (2) 0.7 wt % Cr-tanned; (3) 3 wt % Cr-tanned; (4) 7 wt % Cr-tanned.

was performed for 10 days according to the method of Fujii<sup>19</sup> with some modifications. After the alkaline treatment, the corium pieces were neutralized and washed. The corium pieces were treated to obtain the solution of 6% collagen concentration at pH 3.5 with water and lactic acid.

#### Wet Spinning Condition and Collagen Fiber Spun

The condition of wet spinning is as follows: coagulation bath, acetone; the rate of extractional weight, 19 g/min; the diameter of a hole, 0.35 mm; immersing length, 0.65 m; and winding speed, 2.5 m/min. After wet spinning, these fibers were dehydrated by acetone. Those as-spun fibers were dried at 100°C for 1 h under tension to obtain noncrosslinked fibers.

#### GA Crosslinking, Cr Tanning, and Thermal Treatments

The as-spun fibers were immersed in 0.1, 0.3, and 3.0 wt % GA solution for 30 min at 25°C, respectively. The NaCl concentration of the solutions was 10 wt %. Before immersing the fibers, the pH of GA solutions was adjusted to pH 4.5 by 0.1N NaOH. After GA crosslinking, these fibers were washed and dehydrated by acetone and then dried at 100°C for 1 h under tension. The fibers were immersed in 0.7, 3.0, and 7.0 wt % Cr solution for 4 h, respectively. The Na<sub>2</sub>SO<sub>4</sub> concentration was 3 wt %. The pH of the tanning solutions was not adjusted. The treatment after Cr tanning was same as that of GA-crosslinked fiber. Thermal treatments of noncross-linked, 3 wt % GA-crosslinked, and 7 wt % Cr-tanned fiber were carried out in the dryer at 100, 140, and 170°C for 30 min under no tension. The

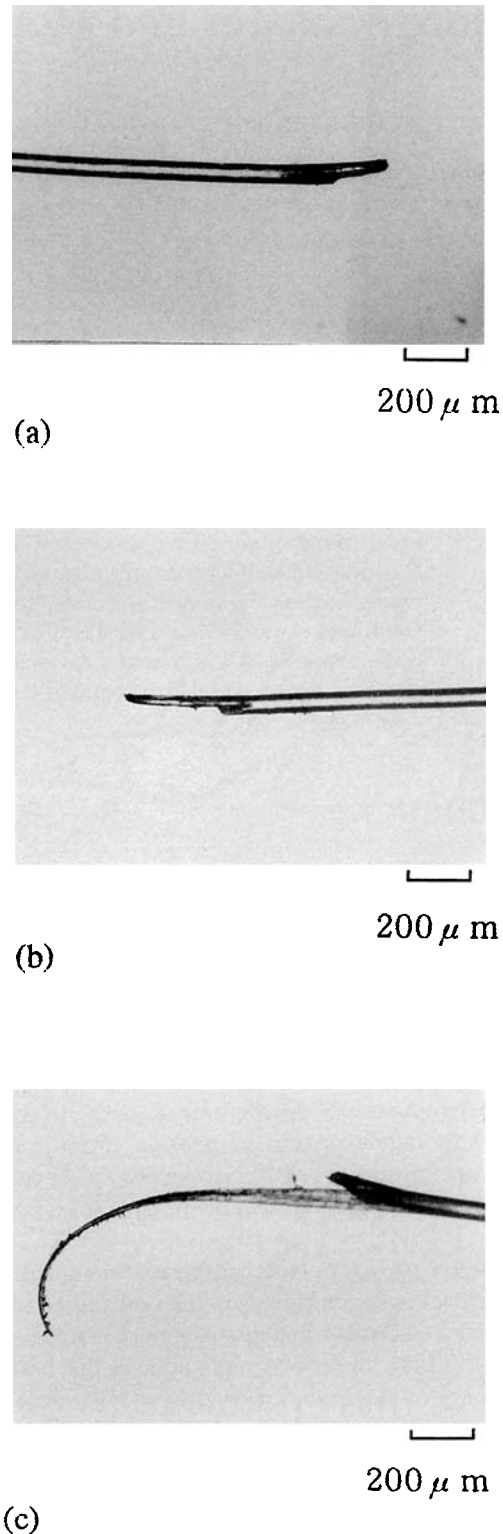


**Figure 2** The optical micrographs of fracture morphology after tensile tests: (a) noncrosslinked fiber; (b) 3 wt % GA-crosslinked fiber; (c) 7 wt % Cr-tanned fiber.

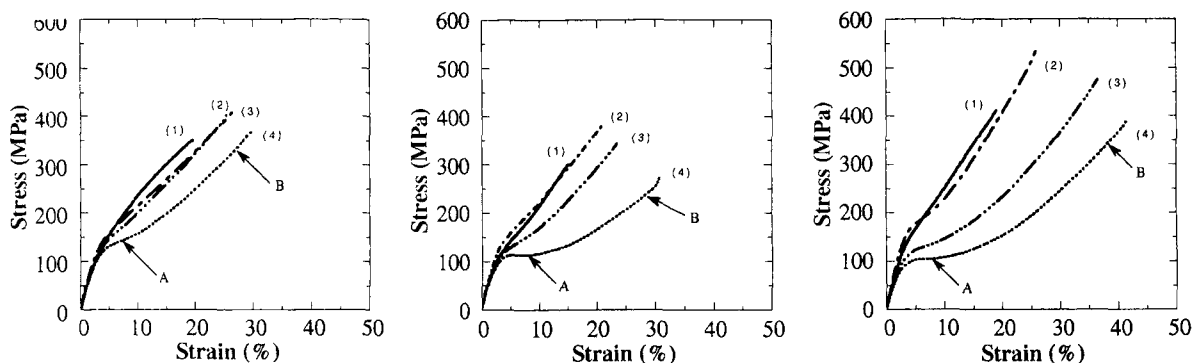


**Figure 3** The stress–strain curves of (a) noncrosslinked, (b) 3 wt % GA-crosslinked, and (c) 7 wt % Cr-tanned fibers before and after thermal treatments: (1) before thermal treatment; (2) after thermal treatment at 100°C; (3) after thermal treatment at 140°C; (4) after thermal treatment at 170°C.

tests were performed at 23°C and 65% RH after conditioning for more than 24 h.

### Tensile Tests

The cross-sectional shape of the fibers is nearly circular and the average diameter of the fibers was determined using an optical microscope. The tensile tests for the fibers were carried out using a UMT-4 tester (Toyo Sotkki Co., Japan) with a crosshead speed of 1 mm/min. The gauge length of the specimen was 20 mm. The fibers were dried under a reduced pressure for more than 48 h after the tensile tests and were coated with a thin layer of gold after drying and examined under a scanning electron microscope.

### Wide-angle X-ray Measurement (WAXD)

WAXD studies were done using Rigaku Denki Model RAD-rA X-ray diffractometer. The X-ray source was nickel-filtered  $\text{CuK}\alpha$  ( $\lambda = 1.54 \text{ \AA}$ ) radiation (50 kV, 200 mA). The diffraction intensity curves of equatorial and meridian directions were obtained by scanning the scintillation counter from  $2\theta = 3^\circ$ – $60^\circ$  by  $1^\circ/\text{min}$  by the transmission method. The degree of orientation was estimated from the half-width of the diffraction peak which was obtained by rotating the fibers from  $90^\circ$  to  $270^\circ$  by  $8^\circ/\text{min}$ .

### Thermal Analysis

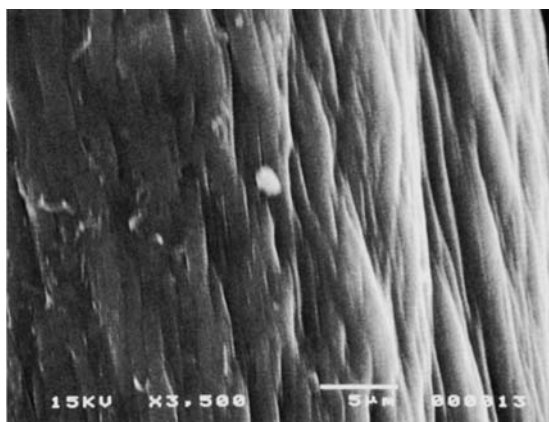
Thermogravimetric (TG) analysis was done using a Seiko TG/DSC 220 to estimate the water content for the fibers. The reference of TG was aluminum oxide. TG analysis was done using an open cell at a

heating rate of  $20^\circ\text{C}/\text{min}$  under dry air at a flowing rate of 300 mL/min from 25 to  $600^\circ\text{C}$ . Differential scanning calorimetry (DSC) analysis was done using Seiko TG/DSC220.<sup>18,20–22</sup> The sample in a sealed cell was immersed more than 24 h. The reference of DSC was demineralized water. DSC was performed at a heating rate of  $2^\circ\text{C}/\text{min}$  under nitrogen gas of a flowing rate of 50 mL/min from 0 to  $200^\circ\text{C}$ .

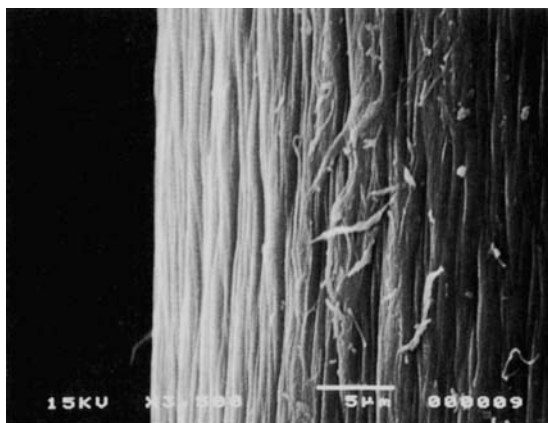
## RESULTS AND DISCUSSION

Figure 1 shows the stress–strain curves of the fibers. As can be seen from this figure, GA-crosslinking and Cr-tanning treatments influence the strain level after yield, and the stress–strain curves shift toward the stress axis with increasing concentration of GA-crosslinking and Cr-tanning agents. Tensile strength and elongation of GA-crosslinked fibers decreased with increasing concentration of the GA-crosslinking agent, and these results agree well with the previous reports.<sup>5,6</sup> On the other hand, the tensile strength and the elongation of Cr-tanned fibers increased with increasing concentration of the Cr-tanning agent.

Figure 2 shows the optical microphotographs of the fractured specimens of noncrosslinked, 3 wt % GA-crosslinked, and 7 wt % Cr-tanned fibers, respectively. All fibers show that the longitudinal splitting occurs along the fiber axis, and the length of the splitting is longer than the diameter of the fiber, similar to that of RTT<sup>14,15</sup> or poly-*(p*-phenylene benzobisthiazole) (PBT) fiber, which is also composed of rodlike molecules.<sup>23,24</sup> It is generally known that both GA-crosslinking and Cr-tanning treatments can improve resistance to water. However, the dependence of the tensile strength and



(a)



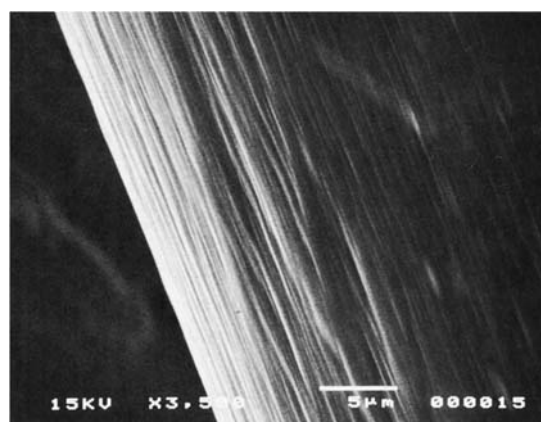
(b)

**Figure 4** The SEM observations on the fiber surfaces of noncrosslinked fibers after thermal treatments of 170°C: (a) at point A after yield; (b) at point B just before break.

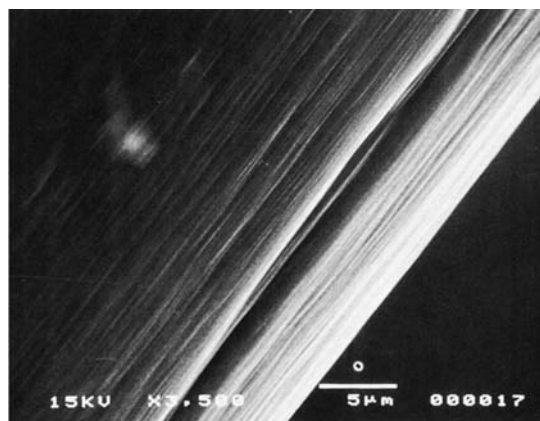
elongation of the fibers on the concentration of GA-crosslinking and Cr-tanning agents is the opposite. It is generally known that both GA crosslinking and Cr tanning can improve resistance to water. However, the dependence of the tensile strength and elongation at break on the concentration of GA-crosslinking and Cr-tanning agents is the opposite.

Figure 3(a)–(c) shows the stress–strain curves of noncrosslinked, 3 wt % GA crosslinked, and 7 wt % Cr-tanned fibers before and after thermal treatments, respectively. The thermal treatment affects remarkably the strain level above the yield point for all kinds of fibers. The stress–strain curves shift toward the strain axis as thermal treatment temperature increases.

Figures 4–6 show the SEM microphotographs of the fractured longitudinal sections and the surfaces of noncrosslinked, 7 wt % Cr-tanned, and 3 wt % GA-crosslinked fibers after thermal treatment at 170°C corresponding to point A above the yield point and to point B just before break on the stress–strain curves, respectively. In Figure 4(a), the straight lines both along the fiber axis and inclined to the fiber axis are observed for the noncrosslinked fibers. The straight lines inclined to the fiber axis are observed at broad intervals from 1 to 3 μm. In Figure 4(b), only the lines along the fiber axis are observed at narrow intervals from 0.3 to 1 μm. Further, the longitudinal splitting and thin separated fibrils can be observed.



(a)

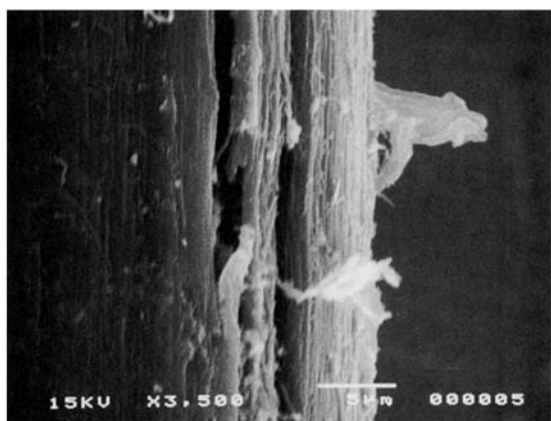


(b)

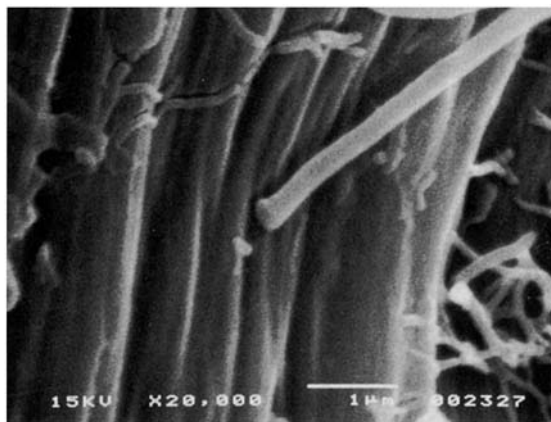
**Figure 5** The SEM observations on the fiber surfaces of 7 wt % Cr-tanned fibers after thermal treatments of 170°C: (a) at point A after yield; (b) at point B just before break.



(a)

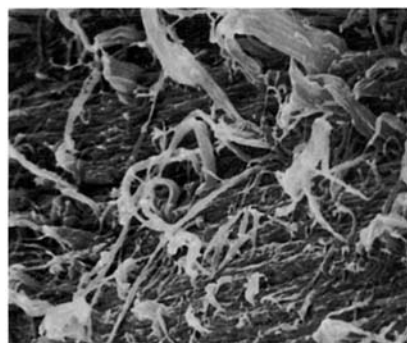


(b)

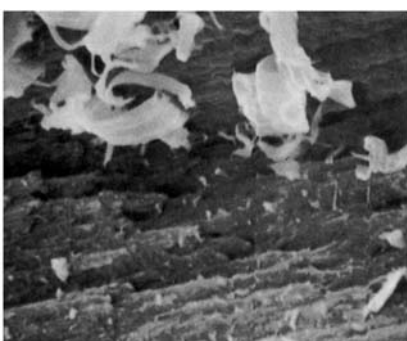


(c)

**Figure 6** The SEM observations on the fibers surfaces of 3 wt % GA-crosslinked fibers after thermal treatments of 170°C: (a) at point A after yield; (b) at point B just before break; (c) at point B just before break.

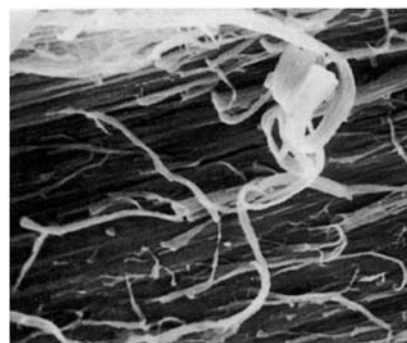


(a) 5 μm



(b)

5 μm



(c)

5 μm

**Figure 7** The SEM observations on the fractured longitudinal section after thermal treatment at 170°C: (a) noncrosslinked fiber; (b) 3 wt % GA-crosslinked fiber; (c) 7 wt % Cr-tanned fiber.

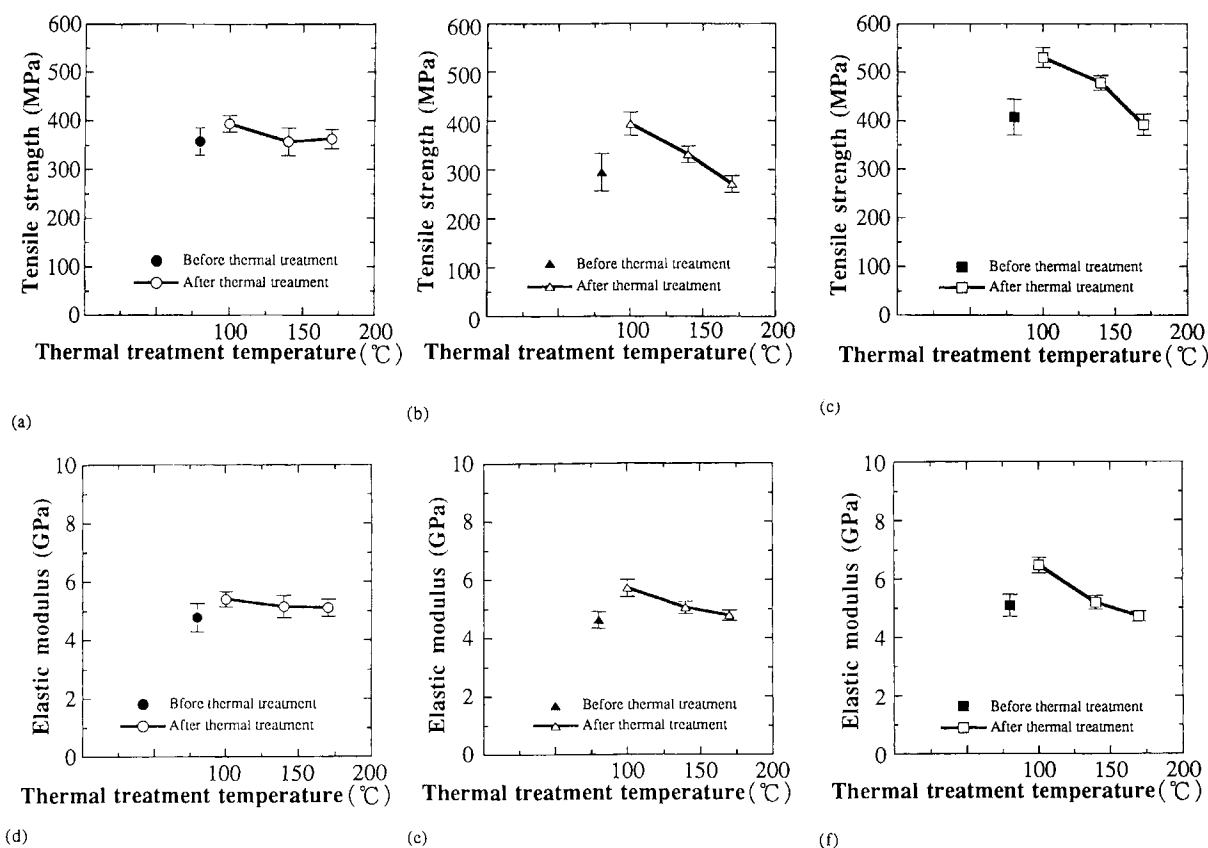


**Figure 8** The effects of treatment temperature on the tensile strength and elastic modulus of the fibers. Tensile strength: (a) noncrosslinked fiber; (b) 3 wt % GA-crosslinked fiber; (c) 7 wt % Cr-tanned fiber. Elastic modulus: (d) noncrosslinked fiber; (e) 3 wt % GA-crosslinked fiber; (f) 7 wt % Cr-tanned fiber.

In Figure 5(a) and (b), the lines which are similar to those of noncrosslinked fiber are also observed for Cr-tanned fibers. The lines at the A point have narrower intervals from 0.3 to 1  $\mu\text{m}$  than those of noncrosslinked fibers. In Figure 5(b), the longitudinal splittings are also observed, but the thin separated fibrils are not observed. In Figure 6(a), the longitudinal splitting and many separated thick fibrils from 1 to 8  $\mu\text{m}$  are observed for GA-crosslinked fiber. In Figure 6(b), the lines along the fiber axis have narrow intervals of 0.3  $\mu\text{m}$ . As can be seen in Figure 5(c), much longitudinal splitting occurs at more microscopic levels. The morphology of fiber surfaces is almost similar to those of noncrosslinked and Cr-tanned fibers shown in Figures 4 and 5. Very thin separated fibrils of 0.05–0.1  $\mu\text{m}$  can be also observed.

Figure 7(a)–(c) shows the SEM microphotographs of longitudinal sections of fractured fibers after thermal treatment at 170°C for noncrosslinked, 3 wt % GA-crosslinked, and 7 wt % Cr-tanned fibers, respectively. The noncrosslinked fibers show both

many thick and thin separated fibrils. The Cr-tanned fibers show many similar fibrils, whereas the GA-crosslinked fibers show only a few separated thick fibrils. The effect of GA-crosslinking and Cr-tanning treatments on the longitudinal fracture morphology is different. The GA crosslinking prevented fibrillation, whereas Cr tanning could not prevent fibrillation.

These SEM observations indicate that the spun collagen fiber after thermal treatment at 170°C consists of many macrofibrils (thick fibrils) which have a diameter of the order of  $10^4$  Å (1  $\mu\text{m}$ ), and this macrofibril consists of fibrils (thin fibrils) which have a diameter of the order of  $10^3$  Å (0.1  $\mu\text{m}$ ). Further, this fibril consists of subfibrils which have a diameter of the order of  $10^2$  Å (0.01  $\mu\text{m}$ ). The results of SEM observations on noncrosslinked fibers after thermal treatment at 170°C clearly indicate that the mechanisms of deformation above the yield point are as follows: First, macrofibrils slipped along the direction inclined to the fiber axis by shear stress; second, many fibrils are elongated with reorientation;

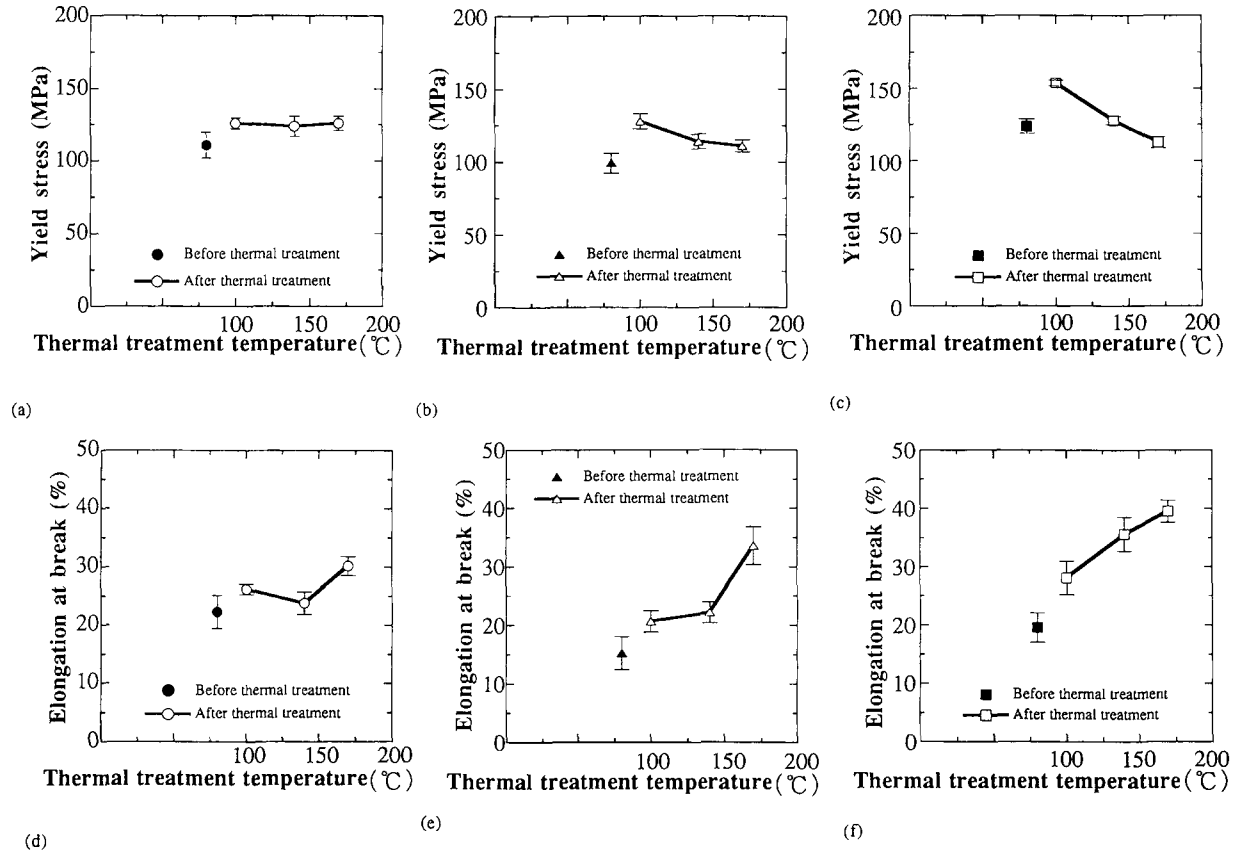


**Figure 9** The effects of treatment temperature on the yield stress and elongation at break of the fibers. Yield stress: (a) noncrosslinked fiber; (b) 3 wt % GA-crosslinked fiber; (c) 7 wt % Cr-tanned fiber. Elongation at break: (d) noncrosslinked fiber; (e) 3 wt % GA-crosslinked fiber; (f) 7 wt % Cr-tanned fiber.

and, finally, longitudinal splitting along the fiber axis occurs, separating fibrils. In the Cr-tanned fibers after thermal treatment at 170°C, slippage of subfibrils plays a more important role after yield than that of macrofibrils, and longitudinal splitting takes place at the boundary of the fibrils. On the other hand, in the GA-crosslinked fibers after thermal treatment at 170°C, longitudinal splitting between macrofibrils plays a more important role than does slippage of macrofibrils.

As above-mentioned, the fibers without thermal treatments showed similar longitudinal splitting along the fiber axis. The longitudinal splitting of these fibers is neither influenced by thermal treatments nor by kind of crosslinking agent. Moreover, the fracture morphology of longitudinal splitting of noncrosslinked, Cr-tanned, and GA-crosslinked fibers before and after thermal treatment is essentially similar to that of dried RTT<sup>15</sup> or PBT fiber.<sup>23,24</sup> However, the SEM observations of fiber surfaces after treatment at 170°C revealed that the process of the longitudinal splitting depends on the kind of

fiber. The Cr tanning promotes the slippage between fibrils immediately after yield. On the other hand, the GA crosslinking brings about the longitudinal

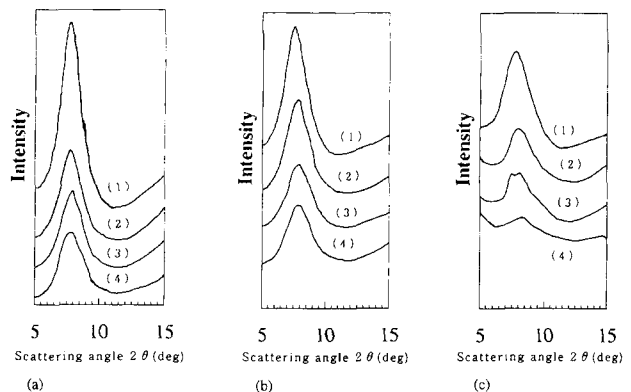


**Figure 10** The X-ray diffraction pattern of the equatorial direction before and after thermal treatment in (a) noncrosslinked, (b) 3 wt % GA-crosslinked, and (c) 7 wt % Cr-tanned fiber. (1) Before thermal treatment; (2) 100°C; (3) 140°C; (4) 170°C.

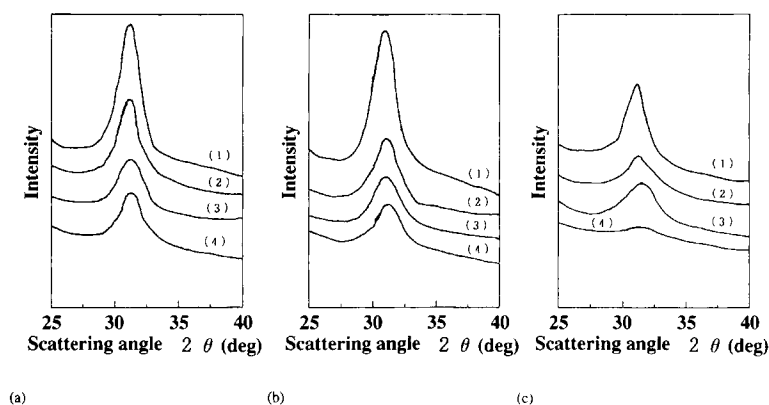


**Figure 11** The X-ray diffraction pattern of the meridian direction before and after thermal treatment in (a) noncrosslinked, (b) 3 wt % GA-crosslinked, and (c) 7 wt % Cr-tanned fiber. (1) Before thermal treatment; (2) 100°C; (2) 140°C; (3) 170°C.

splitting immediately after yield because slippage between macrofibrils or fibrils is prevented.

Figure 8(a)–(f) shows the effects of thermal treatment temperature on the tensile strength and elastic modulus of noncrosslinked, 3 wt % GA-crosslinked, and 7 wt % Cr-tanned fibers, respectively. Figure 9(a)–(f) shows the effects of thermal treatment temperature on yield stress and elongation at break of each fiber. In Figures 8 and 9, the error bars represent the standard deviation. In Figures 8(a) and (d) and 9(a) and (d), the tensile

strength and elastic modulus of noncrosslinked fibers after thermal treatments decrease with increasing temperature, but the elongation increases with increasing temperature. Yield stress is not changed by thermal treatments. In Figures 8(b), (c), (e), and (f) and 9(b), (c), (e), and (f), the tensile strength, elastic modulus, and yield stress of Cr-tanned and GA-crosslinked fibers after thermal treatments decrease with increasing temperature, but the elongation of both fibers increases with increasing temperature.

**Table I** Denaturation Temperature, Enthalpy, and Water Content of Spun Collagen Fibers Before and After Thermal Treatment

Spun Collagen Fibers	Denaturation Temperature (°C)			$\Delta H$ (mJ/mg)	Water Content (%)
	$T_o$	$T_p$	$T_c$		
As-spun collagen fiber	33	43	48	38	15
Noncrosslinked					
Before thermal treatment	33	43	47	37	14
100°C × 30 min	34	41	45	33	13
140°C × 30 min	34	38	42	32	12
170°C × 30 min	33	39	56	12	12
3 Wt % GA-crosslinked					
Before thermal treatment	63	64	67	24	15
100°C × 30 min	62	64	66	24	14
140°C × 30 min	57	58	61	21	13
170°C × 30 min	42	45	50	13	13
7 Wt % Cr-tanned					
Before thermal treatment	87	92	96	26	14
100°C × 30 min	84	87	91	23	14
140°C × 30 min	76	80	84	18	13
170°C × 30 min	63	72	80	12	12

$T_o$ , onset temperature;  $T_p$ , peak temperature;  $T_c$ , conclusive temperature.



Allen et al. reported that tensile strength and the elastic modulus of PBT fiber were improved by thermal treatments below the degradation temperature.<sup>23,24</sup> It is known that material strength is sensitive to structural imperfections such as voids, inclusions, or other flaws. The tensile strength and elastic modulus of each fiber after the treatment at 100°C are higher than those before thermal treatment. The standard deviations of the treated fibers are smaller than those before thermal treatment. Moreover, the diameter of the treated fibers is smaller than that before thermal treatments at 100°C. These results indicate that a decrease of the defects such as voids by thermal treatment at 100°C leads to an increase of tensile strength and elastic modulus as compared with those before thermal treatments. However, the strength enhancements of the fibers treated above 140°C are smaller than those treated at 100°C. The thermal treatments show the maximum effect at 100°C.

Figures 10 and 11 show the X-ray diffraction pattern of the equatorial and meridian direction of noncrosslinked, 3 wt % GA-crosslinked, and 7 wt % Cr-tanned fibers before and after thermal treatment, respectively. An increase of treatment temperature leads to more broad peaks at  $2\theta \doteq 31^\circ$  and  $2\theta \doteq 7.5^\circ$ , corresponding to a residue repeat distance and distance between collagen molecules, respectively. Yamamoto et. al. suggested that the conformation of a triple helix would be destroyed due to ruptures of interhelical hydrogen bonds by thermal treatment above 160°C for dried RTT.<sup>12</sup> It is known that the diffraction pattern of hot-cast gelatin film in the state of random coil does not show a peak at  $2\theta \doteq 31$ , corresponding to a residue repeat distance. The results of the diffraction pattern clearly indicate that gelatinization takes place due to an increase of treated temperature. The degree of orientation of the fibers slightly decreases with an increase of treated temperature, but the fibers keep still high orientation above 70%.

Table I shows the results of TG and DSC, in which water content, denaturation temperature, and enthalpy of noncrosslinked, 3 wt % GA-crosslinked and 7 wt % Cr-tanned fibers before and after thermal treatments are shown. The sample weight of all fibers in the TG curves decreased with increasing temperature and reached a stationary value at about 185°C and then extremely decreased above 185°C. The water content of all fibers, which lie in the region from 12 to 15%, is estimated from the weight loss at this stationary value. It is known that water acts as a plasticizer for collagen. However, the result that the elastic modulus decreases with increasing

temperature suggests that other factors are more important. As can be seen from Table I, the denaturation temperature ( $T_0$ ,  $T_p$ , and  $T_c$ ) and enthalpy of as-spun collagen fiber is almost the same as those of noncrosslinked fiber before thermal treatment. These results indicate that gelatinization hardly occurred by this treatment.

In case of the GA-crosslinked and Cr-tanned fibers, denaturation temperature ( $T_0$ ,  $T_p$ , and  $T_c$ ) and enthalpy decrease with increasing treated temperature. In noncrosslinked fiber,  $T_0$  keeps a constant value after thermal treatments, but  $T_p$  also decreases with increasing treated temperature. However,  $T_c$  after thermal treatment at 170°C is higher than that before thermal treatment. These changes suggest that collagen is covalently crosslinked by thermal treatments, but the increase in elongation at break and the decrease in elastic modulus with increasing treated temperature indicate that gelatinization plays a more important role than does the effect of crosslinking. The denaturation enthalpy of all fibers decreased with increasing treated temperature. This indicates that, although thermal treatment brings about gelatinization, collagen does not perfectly change to gelatin of the random coil state. This is also supported by WAXD results in which the fibers treated at 170°C still show a peak at  $2\theta \doteq 31^\circ$  in the meridian direction and high orientation above 70%.

Thus, the results of DSC agree well with those of WAXD: These results indicate that thermal treatments lead to the gelatinization result in the disorder of lateral molecular interactions. These gelatinated regions in the fibers play an important role in the tensile deformation after the yield point, in which slippage and separation of microfibrils and/or fibrils predominantly occur. The thermal treatments have two effects in fracture behavior: One is a decrease of the defects such as voids; the other is the gelatinization. The effect of a defect decrease plays a more important role in the treatment at 100°C to improve the tensile properties, whereas the gelatinization plays a more important role in the treatment above 140°C than that of enhancing the tensile strength.

## CONCLUSIONS

The promotion of GA crosslinking reduced tensile strength and elongation, whereas the promotion of Cr tanning enhanced these properties. However, the fracture morphology in which longitudinal splitting occurs is independent of the kind of crosslinking.

The SEM observations showed that the spun collagen fiber after the thermal treatment at 170°C

consists of many macrofibrils which have a diameter of the order of  $10^4$  Å, and this macrofibril consists of fibrils which have a diameter of the order of  $10^3$  Å. Further, these fibrils consists of subfibrils which have a diameter of the order of  $10^2$  Å. In the case of noncrosslinked fibers treated at 170°C, the process of deformation above the yield point is as follows: First, the macrofibrils slip along the direction inclined to the fiber axis by shear stress components; second, many fibrils are elongated with reorientation; and, finally, longitudinal splitting along the fiber axis occurs by separation between the fibrils. Although all fibers showed splitting fracture, the splitting process depended on the kind of crosslinking. Cr tanning enhanced the slippage between fibrils immediately after yield, whereas GA crosslinking brought about longitudinal splitting immediately after yield, preventing the slippage between macrofibrils or fibrils. Therefore, noncrosslinked and Cr-tanned fibers split with fibrillation, whereas GA-crosslinked fibers split without fibrillation.

The thermal treatments have two effects in fracture behavior: One is a decrease of the defects; the other is gelatinization. The effect of a defect decrease plays a more important role in the treatment at 100°C to improve the tensile properties, while gelatinization plays a more important role in the treatment above 140°C. The gelatinization brings about the disorder of lateral molecular interactions and this results in the enhancement of slippage and separation of macrofibrils and/or fibrils after the yield point.

## REFERENCES

1. T. Miyata, *Kobunshi*, **19**(218), 355 (1970).
2. M. Yoshida, *Chem. Today*, **Oct.**, 26 (1990).
3. A. Utsuo, *J. Text. Machin. Soc. Jpn.*, **26**, 207 (1973).
4. A. Utsuo, *Hikaku Kagaku*, **20**(4), 209 (1975).
5. W. C. Schimpf and F. Rodriguez, *Ind. Eng. Chem. Prod. Res. Dev.*, **16**(1) (1977).
6. F. Rodriguez, *Polym. News*, **9**, 262-265 (1984).
7. J. H. Bowes and C. W. Cater, *J. Appl. Chem.*, **15**, 296 (1965).
8. I. V. Yannas, *J. Macromol. Sci. Rev. Macromol. Chem.*, **C7**(1), 49 (1972).
9. J. C. W. Chien, *J. Macromol. Sci. Rev. Macromol. Chem.*, **C12**(1), 1 (1975).
10. H. Okamura, *Kobunshi*, **17**(198), 888 (1968).
11. I. V. Yanns and C. Hung, *J. Polym. Sci. Part A-2*, **10**, 557 (1972).
12. Y. Yamamoto, Y. Saito, and S. Kinoshita, *Sen-i Gakkaishi*, **40**(1), 90 (1984).
13. Y. Saito, N. Nakajima, and Y. Yamamoto, *Sen-i Gakkaishi*, **41**(10), 44 (1985).
14. R. C. Haut, *J. Biomech.* **19**(11), 951 (1986).
15. V. Arumugam, M. D. Naresh, N. Somanathan, and R. Sanjeevi, *J. Mater. Sci.*, **27**, 2649 (1992).
16. G. Harmed and F. Rodriguez, *J. Appl. Polym. Sci.*, **19**, 3299 (1975).
17. M. Taniguchi, *Kobunshi*, **12**, 608 (1963).
18. S. Nakazaki, K. Takaku, M. Yuguchi, H. Edamatsu, and K. Takahashi, *Anim. Sci. Technol.*, **65**(11), 1018 (1994).
19. T. Fujii, *Z. Physiol. Chem.*, **350**, 1257 (1969).
20. K. Takahashi and M. Hattori, *J. Food Sci.*, **58**(4), 734-738 (1993).
21. Y. Nomura, K. Takahashi, and K. Shirai, *Anim. Sci. Technol.*, **65**(1), 33 (1994).
22. K. Takahashi and M. Hattori, *Biosci. Biotech. Biochem.*, **58**(1), 178 (1994).
23. S. R. Allen, R. J. Farris, and E. L. Thomas, *J. Mater. Sci.*, **20**, 4583 (1985).
24. S. R. Allen, R. J. Farris, and E. L. Thomas, *J. Mater. Sci.*, **20**, 2727 (1985).

Received March 17, 1995

Accepted August 3, 1995